 doi:10.20944/preprints202205.0396.v1

Customizable collagen vitrigel scaffolds and preliminary results in corneal engineering

María Dolores Montalvo-Parra [1, 2]
dolores.montalvo@tec.mx
Wendy Ortega-Lara[1]
wlortega@tec.mx
Denise Loya-García[2]
deniseloyagarcia@tec.mx
Andrés Bustamante-Arias[2]
abustamante.eye@gmail.com
Guillermo-Isaac Guerrero-Ramírez[2]
g.querrero.guillermo@gmail.com
Cesar E. Calzada-Rodríguez[2]
c.calzada96@gmail.com
Guiomar Farid Torres Guerrero[2]
A01374681@itesm.mx
Betsabé Hernández-Sedas[2]
betsyhs18@gmail.com
Italia Tatnaí Cárdenas-Rodríguez[2]
italiatatnai@gmail.com
Sergio E. Guevara-Quintanilla[2]
sergio.gq.95@gmail.com
Marcelo Salán-Flores[2]
marcelosalan@gmail.com
Miguel Ángel Hernández-Delgado[2]
dr.miguelhdezd@gmail.com
Salvador Garza-González[2]
sagarza95@gmail.com
Mayra G. Gamboa-Quintanilla[2]
mayragamboaq@gmail.com
Luis Guillermo Villagómez-Valdez[2]
memovillagomez@gmail.com
Judith Zavala[2]*
judith.zavala@tec.mx
Jorge E. Valdez-García[2]
jorge.valdez@tec.mx

[1] Tecnologico de Monterrey, Escuela de Ingenieria. 2501 Garza Sada Ave. Colonia Tecnologico. C.P. 64849. Monterrey, N.L., Mexico.
[2] Tecnologico de Monterrey, Escuela de Medicina. 3000 Morones Prieto Ave. Colonia Los Doctores. C.P. 64710. Monterrey, N.L., Mexico.
*Corresponding author

 doi:10.20944/preprints202205.0396.v1

Abstract

We set a feasible method to produce tailored collagen scaffolds and analyzed its potential for corneal engineering.

Collagen-vitrigel membranes (CVM) were produced with a 1:1 ratio of Dulbecco's Modified Eagle's medium (DMEM), 1% antibiotics and 8% fetal bovine serum, and 5mg/mL collagen type I. Three volumes of collagen were used: 1X (2.8 $\mu L/mm^2$ of collagen), 2X, and 3X. Vitrification was done at 40% relative humidity (RH), 40° C, and 30 rpm using a matryoshka system set with a shaking-oven and a desiccator with a saturated K_2CO_3 solution. The CVM was characterized for width, microstructure, transparency, and biocompatibility using NIH3T3 cells. Surgical manipulation was assessed in an *ex vivo* corneal model. Constructs of corneal endothelial cells (CECs) and 2X-CVM were transplanted into five 18-month-old White New Zealand rabbits.

CVM exhibited homogeneous surface and laminar organization. Membrane width increased with gel volume from 3.65µm to 7.2µm. 1X and 2X-CVM exhibited a 99% transmittance. NIH3T3 cells concentration increased 3-fold within 48 h with no significant difference among the 3 CVM ($p = 0.323$). The 2X-CVM was surgically manipulable. Transplantation of corneal endothelial cells (CECs) seeded over 2X-CVM restored corneal endothelium.

The matrioshka system is a feasible method that yields CVM suitable for corneal engineering.

Keywords: scaffold, collagen vitrigel, tissue engineering, cornea, corneal endothelium

 doi:10.20944/preprints202205.0396.v1

Introduction

Tailoring scaffolds for organ design and reconstruction via tissue engineering represents an important breakthrough that may alleviate the organ and tissue scarcity reported by the World Health Organization[1], [2]. Collagen type I has great potential for tissue engineering because it possesses low immunogenicity, produces porous structures, allows permeability, has good biocompatibility, and it is biodegradable [3]. It is widely distributed in the human body as part of the most abundant protein in the extracellular matrix and their functions in promoting cell adhesion and migration.

Collagen scaffolds are produced following a wide range of methodologies that vary in three main aspects: 1) methodology, including desiccation, freeze drying, electrospinning, and 3D printing; 2) conditions, like the collagen source and concentration, polymerization pH, and temperature; and 3) characterization, including microstructure, transmittance, FTIR, X-Ray diffraction, cell adhesion, water uptake, biodegradability, and *in vivo* biocompatibility [4]–[6]. This leads to marked variation in parameters that set their potential to be applied for clinical purposes, like the mechanical strength, stability, and biocompatibility. For this, there is a limited reproducibility of the methodologies and their application in tissue engineering [7].

Overall, the main challenges on producing collagen scaffolds for tissue engineering are the mechanical properties and biocompatibility. The blending of collagen with polymers or nano-inorganic materials improves its mechanical properties that enables their use as platform for nerve regeneration, bone repair, tendon reconstruction, vascular grafts, and skin [8]–[12]. This can be achieved using electrospinning, 3D printing, tissue decellularization, lyophilization, and freeze-drying techniques. However, blended products must be studied carefully for their degradability, as some of the products might play a role in enhancing immune response in the host.

Enhancing the cross-linking of collagen fibers in the scaffolds is an alternative strategy for the improvement of their mechanical properties while maintaining their low immunogenicity. Ultra-violet (UV) light treatment and desiccation in specific conditions are used for this purpose, producing vitrified scaffolds. Given that these strategies can produce transparent membranes, they have great potential for the restoring of ocular tissues like the cornea [13]–[15]. Currently, the protocols to produce collagen-vitrigel membranes (CVM) vary in the conditions of temperature, time of desiccation, relative humidity, etcetera. This results in the variation of the desired characteristics like thickness, fiber diameter, density, and organization; that affect their application in translational research.

In this research, we provide a simple and reproducible method to produce CVM, that can be tailored to produce membranes with different characteristics with potential use for corneal engineering. This way, we are closing the gap among the methods, leading to the development of standardized protocols that yield reproducible and quantitative characterization, that in turn facilitate comparative research and development of prototypes for clinical applications [16][17].

2. Methods

2.1 Matryoshka system assembling for the production of collagen membranes

For the manufacturing of CVM, a matryoshka system was assembled (Figure 1a). It consisted of an incubator with a steady temperature (T) bearing a desiccator with a saturated K_2CO_3 solution to control the RH. For this purpose, 50 mL of K_2CO_3 solution were prepared using 1.15 g of K_2CO_3 (Sigma-Aldrich, P5833, St. Louis, Missouri, USA) per milliliter of bidistilled water. The salt

Preprints (www.preprints.org) | NOT PEER-REVIEWED | Posted: 30 May 2022 doi:10.20944/preprints202205.0396.v1

solution was placed in a 200 mL beaker and fixed onto a 330 × 246 × 262 mm desiccator with a clear plastic dome (Thermo Scientific Nalgene, 5310-0250, Cleveland, Ohio, USA). A closed system was created by placing the sealed desiccator inside a shaking-plate incubator (I5211DS; Labnet International, Edison, New Jersey, USA) (Figure 1 a). The T and shaking speed of the incubator were set to 40°C and 30 rpm, respectively. Shaker function was turned on 48 h after the gel was placed inside the matryoshka system, to avoid gel tilting. T and RH were measured with a Monitoring Traceable Hygrometer (4040CC; Traceable® Products, Webster, Texas, USA) placed inside the desiccator. T and RH were registered daily until a temperature of 40°C and an RH of 40% were recorded consistently for ~7 days. During this period, no sample was placed inside the system.

2.2 Collagen-based membrane production

2.2.1 Collagen gel preparation

CVM production was based on methods described previously [13], [14]. Advanced Dulbecco's Modified Eagle's medium (DMEM) (Gibco–Thermo Fisher Scientific, Grand Island, New York, USA) was prepared with 1% penicillin–streptomicyn (Gibco) and 8% qualified fetal bovine serum (Gibco) and kept on ice. Subsequently, 22 mM HEPES (Gibco) was added and mixed with a cold type-I collagen solution (5 mg/mL) at a 1:1 ratio (Gibco) until a uniform yellow mixture was obtained by gentle pipette resuspension. The pipettes were also kept on ice, to avoid early gelation. Twelve-well plates were used as casts for 2.2 mL of the collagen mix (2.8 μL/mm^2 of collagen; 1x volume). Gel casts were also prepared at volumes of 2x and 3x collagen. The plates containing the collagen mix were placed in an MCO-18AIC incubator (Sanyo, Osaka, Japan) and kept at 37°C, 5% CO_2 for 2 h, until gelation.

2.2.3 Desiccation

Plates containing collagen gels were placed inside the matryoshka system. The temperature and shaking speed of the incubator were set at 40°C and 30 rpm, respectively. The system remained closed, and T and RH were registered daily. Around day 10–13, the volume of the collagen gels decreased, and membranes were formed. The matryoshka system was then opened and membranes were rinsed with bidistilled water until elimination of the phenol red in the medium. The samples were placed back inside the system, to complete a period of 37 days of incubation.

2.2.4 Membrane rehydration

Plates were removed from the matryoshka system. Bidistilled water was poured into the wells of the plates containing the collagen membranes, left for ~20 min, and removed. The borders of each membrane were lifted using water pressure. Rounded-tip forceps were used to gently pull the remainder of the membranes away from the bottom of the well.

2.3 Collagen-based membrane characterization

Preprints (www.preprints.org) | NOT PEER-REVIEWED | Posted: 30 May 2022 doi:10.20944/preprints202205.0396.v1

2.3.1 Optical microscopy

Membranes were humidified for 20 min and the water excess was then removed. The surface of CVM was observed with an Axiovert 40 CFL contrast microscope (Carl Zeiss Microscopy, Jena, Germany) and photographed.

2.3.2 Scanning electron microscopy (SEM)

Samples of the membranes were coated with gold using a Quorum QR150 ES sputtering system (Quorum Technologies, Laughton, United Kingdom). The surface and transversal ultrastructure was observed and measured with an EVO MA Scanning Electron Microscope (Carl Zeiss Microscopy). Moreover, the fibers of samples that were desiccated for 7 days (4 samples, 34 fibers per sample) were photographed and measured using NIH ImageJ. Briefly, image calibration to microns was performed, followed by selection of linear regions of interest and accumulation using the *Analysis>>Measure* route in the ImageJ software.

2.3.4 3D confocal microscopy

Surface regularity and sample thickness were assessed in triplicate using an Axio-CSM 700 50x objective (Carl Zeiss Microscopy). Samples were hydrated for 20 min prior to data collection.

2.3.5 In vitro cell adherence, viability, and cytotoxicity

The NIH3T3 cell line was obtained from ATCC (CRL-1658™). CVM were cut into circles of 5 mm diameter to fit a 96-well plate. CVM were sterilized with Microdacyn (Oculus Innovative Sciences, CA, USA) and rinsed with sterile water. Water was removed and membranes were left to dry and adhere to the bottom of the wells. NIH3T3 cells were seeded (~10,000) in 100 µl of DMEM F12 (12491-015; Gibco) and incubated overnight at 37°C, 5% CO_2.
A cytotoxicity and viability test were performed using Cell Titer Blue (Promega, Madison, WI, USA) according to the manufacturer's instructions. Briefly, 20 µl of Cell Titer Blue were added to each experimental, assay control, and sample control well, followed by gentle resuspension and incubation at 37°, 5% CO_2 for 2 h. The same conditions were used to perform a 2–50 x 10^3 cell fluorescence ladder comparison. Fluorescence was recorded on a Synergy HT spectrophotometer (BioTek, Winooski, VT, USA). Triplicates were tested for each membrane concentration in the experimental condition (membrane + cells), the sample control condition (cells alone), the negative control condition (membrane alone), and the assay control condition (medium + Cell Titer Blue).

2.3.6 Fourier-transformed infrared spectra (FTIR)

Functional groups were identified on each membrane sample using an infrared spectrophotometer coupled with a Fourier transform Spectrum 400 apparatus (Perkin Elmer,

Preprints (www.preprints.org) | NOT PEER-REVIEWED | Posted: 30 May 2022 doi:10.20944/preprints202205.0396.v1

Waltham, MA, USA) and recorded in the wavenumber range of 4000–400 cm−1 at room conditions.

2.3.7 Transmittance analysis

Absorbance was acquired throughout UV–VIS spectra (380–700 nm) using a Synergy HT spectrophotometer (BioTek, Winooski, VT, USA) and transformed to transmittance using the Beer–Lambert law equation. Experiments were performed in triplicate.

2.3.8 X-Ray diffraction analysis (XRD)

XRD was used to assess the crystallinity of the CVM. XRD was recorded in the 2θ range, between 10° and 85°, with a step size of 0.026 using a PANalytical Empyrean diffractometer (PANalytical, Almelo, Netherlands) and CuKα radiation (λ = 1.5406 Å). The voltage applied was 45 kV and the current was 40 mA.

2.3.9 Ex vivo surgical manipulation test

To analyze the ease for surgical manipulation of the CVM, an ex-vivo model was used. Cow eyes from local butcher shop were fixated over styrofoam plates. 1X, 2X, and 3X membranes were used for Descemet's stripping endothelial keratoplasty surgical procedures over the eyes. The surgical procedures were performed by two ophthalmologist surgeons who subjectively evaluated the ease of manipulation of the membranes.

2.4 Engineered corneal endothelium assembling

This study was approved by the institutional local ethics committee (School of Medicine of Tecnologico de Monterrey), number 2019-003. All animals were treated according to the Guide for the Care and Use of Laboratory Animals adhering to the guidelines for the human treatment and ethical use of animals for vision research stated by the National Institutes of Health guide for the care and use of Laboratory animals. White New Zealand rabbits were housed in individual cages and fed *ad libitum*.

Two 3-month-old male White New Zealand rabbits were used to isolate CECs according to previous methodology [18], [19]. Briefly, White New Zealand rabbits were euthanized with an intravenous pentobarbital lethal dose (90-180 mg/Kg). The endothelium was surgically detached from the corneal stroma and digested with 1 mg/ml of collagenase type I (Sigma-Aldrich Co., St. Louis, MO) at 37 °C for 1 h. The CECs were cultured using OptiMEM-I supplemented with 8% FBS, 20 ng/ml of nerve growth factor (NGF; Sigma-Aldrich Co.), 5 ng/ml of epidermal growth factor (EGF; Sigma-Aldrich Co.), 200 mg/L of calcium chloride (Sigma-Aldrich Co.), 20 μg/mL of ascorbic acid (Sigma-Aldrich Co.), 0.08% chondroitin sulfate (Sigma-Aldrich Co.), and 1% antibiotics until confluency. A passage was done, and the CECs were cultured using basal media OptiMEM-I supplemented with 8% FBS and 1% antibiotics until confluency. A second passage

Preprints (www.preprints.org) | NOT PEER-REVIEWED | Posted: 30 May 2022 doi:10.20944/preprints202205.0396.v1

was done, and the CECs were seeded over 2X-CVM (according to the results of the *ex vivo* model) at a density of 2500 cells/mm^2 overnight. The CECs/CVM construct was analyzed by light microscopy to register cell polygonal morphology and cell adherence.

2.5 Pilot study of the transplantation of engineered corneal endothelium in an animal model

Five 20-month-old male White New Zealand rabbits were used for corneal damage model, according to a previous study [20]. Local and general anesthesia was applied using tetracaine (Ponti Ofteno, Laboratorios Sofía, Jalisco, Mexico) and intramuscular 30 mg/Kg ketamine and 5 mg/Kg xylazine, respectively. Two paracenteses were made, and an anterior chamber maintainer was introduced. Descemethorexis was performed and transplantation of the CECs/CVM constructs was done in 4 eyes (experimental group). Three eyes were transplanted using only collagen membrane (control group). Post-surgical analgesic and antibiotic scheme were conducted using topic Dexamethasone (Soldrin, Pisa, Guadalajara, Jalisco) 1 mg/mL, 1 to 2 drops every 8 hours for 48h, subcutaneous Flunixin (Sanfer, CDMX, Mexico) 1-2 mg/Kg every 12h for 3 days, and intravenous Enrofloxacin (Bioquin, BioZoo, Jalisco, Mexico) 5-10 mg/Kg every 8 hours for 7 days. Clinical follow-up and photodocumentation was done daily for 90 days. The rabbits were euthanized with a pentobarbital lethal dose. The corneas were excised and analyzed by light microscopy.

The corneal endothelium was detached and analyzed by immunocytochemistry to analyze the presence of ZO-1 and NA/K-ATPase. Briefly, the corneal endothelium was fixed with cold 4 ºC methanol for 24 h and rinsed 3 times with PBS. Unspecific epitopes were blocked with 5% bovine serum albumin (BSA) (Sigma-Aldrich, Co.) at 37 ºC for 30 min. Primary antibodies, rabbit polyclonal for ZO-1 (Invitrogen, Waltham, MA, USA) 1:100, and mouse monoclonal anti-alpha 1 Na-K/ATPase (Abcam, Cambridge, MA, USA) 1:100, were used. The secondary antibody Alexa 488 (2:500) (Abcam) was used for ZO-1 primary antibody, and Alexa 568 (1:500) (Abcam) for Na-K/ATPase primary antibody. DAPI (Sigma-Aldrich Co.) was used as nuclei counterstain. The images were analyzed using ImageJ software [21].

Statistical analysis

Statistical comparison of the experimental groups was carried out using paired Student's t-tests or analysis of variance (ANOVA). Significance was set at $P < 0.05$. Microsoft Excel (2013; Redmond, WA, USA) and Systat Sigma Plot (V. 11; San Jose, CA, USA) were used for data processing, statistical analysis, and graph generation.

3. Results

3.1 Matryoshka system assembling and stabilization

The temperature inside the system remained constant at 40 °C (SD of ± 0.19 °C at the stabilization phase, and SD of ± 0.64 °C in the presence of the samples). The RH at the stabilization phase ranged from 47% to 42% (SD, ±1.68%), whereas it ranged from 51% to 33% (SD, ± 5.52%) during the sample-desiccation period

Preprints (www.preprints.org) | NOT PEER-REVIEWED | Posted: 30 May 2022 doi:10.20944/preprints202205.0396.v1

(Figure 1b and 1c). A volume of 50 mL of the saturated salt solution lasted for ~100 days when the samples were inside the matryoshka system.

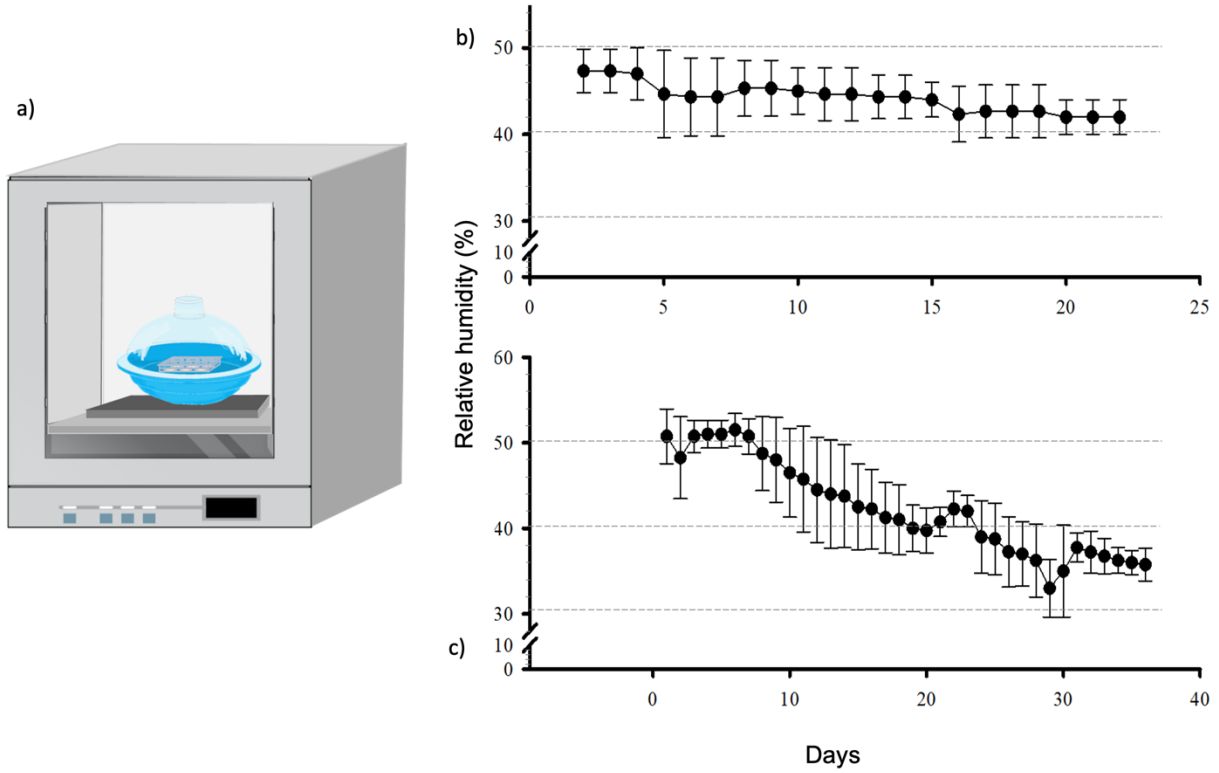

Figure 1. Matryoshka system assemblage (a). Daily behavior of the relative humidity percentage at the stabilization phase (b) and in the presence of 6 mL of collagen gel (c).

3.2 Membrane desiccation and rehydration

The formation of the membranes occurred when the thickness of the collagen decreased to ~1 mm (Figure 2). Gels at 1X collagen concentration required 10–13 days to reach the membrane state, whereas 2X and 3X required approximately 15 and 20 days, respectively. We also observed that phenol red must be removed during the gel-to-membrane transformation, to avoid further interference with transparency. At the end of the 37-day desiccation period, the membranes were completely transparent. Membrane rehydration for ~20 min was necessary to achieve a good retrieval from the cast. A malleable, transparent material was observed in water suspension. The membranes were placed in a water drop on plastic film, the borders were unfolded, and water was removed using a pipette to straighten the membranes, which were left to dry again at room temperature.

Preprints (www.preprints.org) | NOT PEER-REVIEWED | Posted: 30 May 2022 doi:10.20944/preprints202205.0396.v1

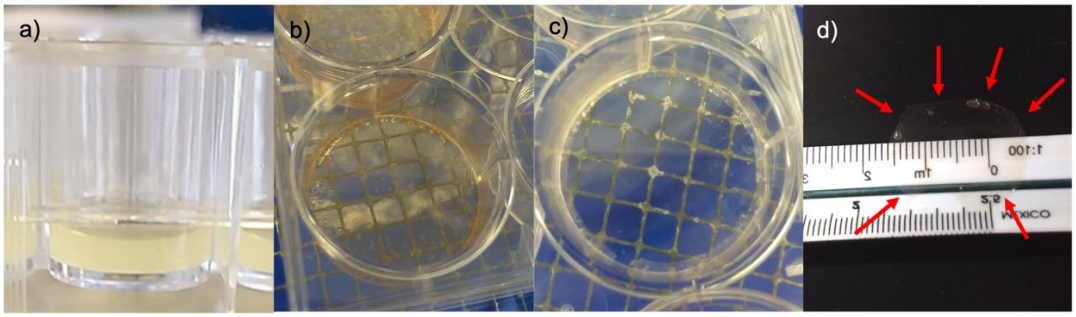

Figure 2. Desiccation process: (a) gel before vitrification, (b) membrane with phenol red; (c) rinsed membrane at day 37; and (d) membrane removed from the cast and dried at room temperature.

3.4 Confocal, optical, and SEM characterization

Confocal microscopy was performed at a width of 3.65 μm for 1X collagen membranes, 4.8 μm for 2X membranes, and 7.2 μm for 3X membranes (Figure 3a, 3b, and 3c).
A homogeneous surface was observed after 37 days of desiccation in the three membrane types (Figure 3d). The average fiber diameter was 1.3 μm (SD ± 0.23). Membrane width increased with collagen concentration and lamina density (Figure 3e, 3f, and 3g).

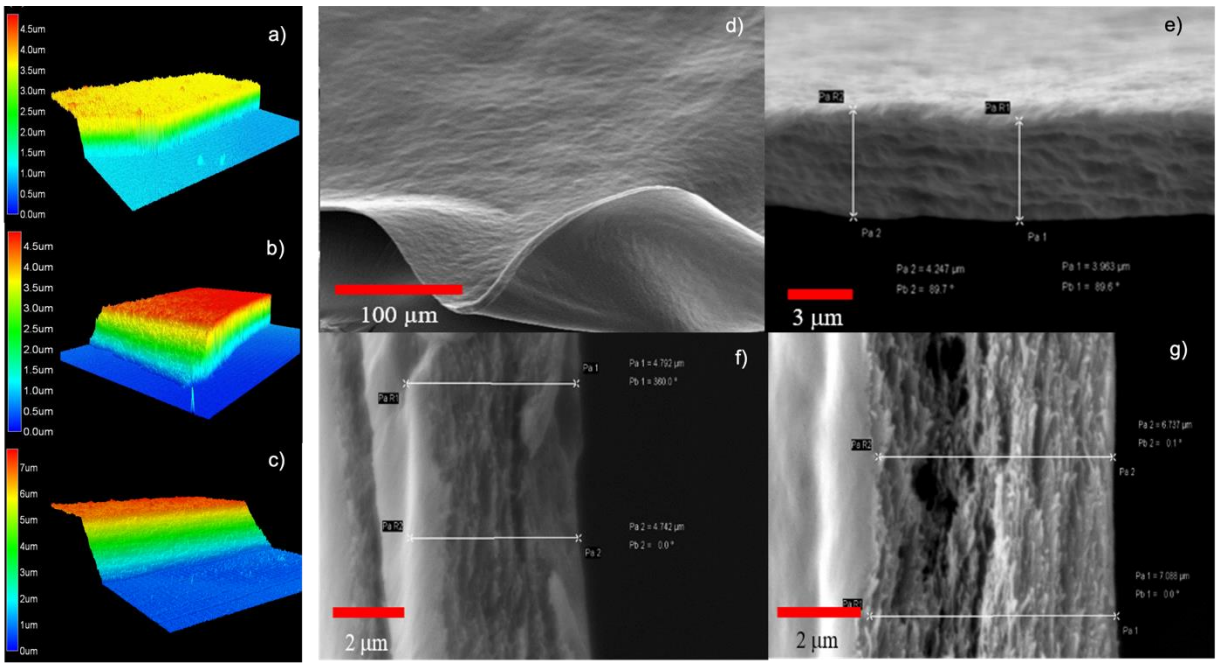

Figure 3. Representative surface and width evaluation using material confocal microscopy: 1X (a), 2X (b), and 3X (c) CVM (n = 3). Surface micrograph of a 37-day desiccated 1X membrane (d). SEM transversal-view micrograph of a 1X (e), 2X (f), and 3X (g) membranes in wet conditions, showing a width of ~3.6, 4.8, and 7.2 μm respectively.

3.7 Membrane characterization: cell viability, IR spectra, transmittance, and X-ray diffraction

NIH3T3 mouse fibroblasts showed adherence to 1X, 2X, and 3X CVM (Figure 4). A fluorescence analysis indicated that the 10 x 10^3 cells that were seeded initially proliferated to ~31.7 x 10^3 cells in wells with no membranes. The populations of cells cultured on 1X, 2X, and 3X CVM increased to ~35.8 x 10^3, ~29.6 x

Preprints (www.preprints.org) | NOT PEER-REVIEWED | Posted: 30 May 2022 doi:10.20944/preprints202205.0396.v1

10^3, and 29.5 x 10^3 cells, respectively. The populations of cells increased by 3-fold within 48 h. One-way ANOVA detected no significant differences between the means of all four samples (P = 0.323, n = 3). However, compared with controls, the populations of cells cultured on 1X CVM increased by 12%.

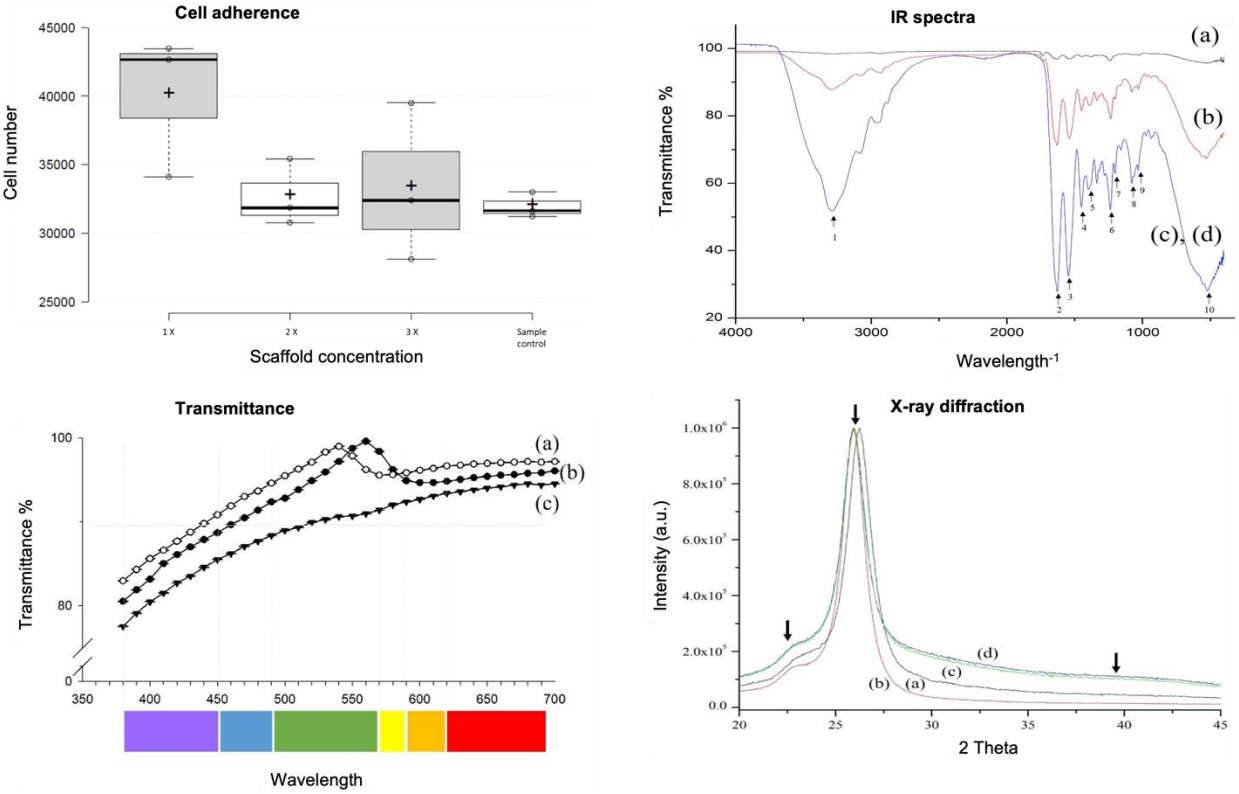

Figure 4. Cell adherence. NIH3T3 cell count at 48 hours when cultured over 1X, 2X and 3X collagen membranes. Sample control lacks of collagen membrane. **IR spectra** of pure collagen type 1 (a), 1X collagen membranes (b), 2X collagen membranes (c), and 3X collagen membranes (d). **Transmittance**. Percent of transmittance of membranes fabricated using varying collagen volumes: 2X (a), 1X (b), and 3X membranes (c). **X-ray diffraction.** Patterns of pure collagen type 1 (a), 1X (b), 2X (c), and 3X collagen (d) membranes. A 0.6° offset was introduced to detect each pattern clearly. The arrows indicate the 22°, 25.9°, 39.8° humps for amorphous collagen and the two hydroxyapatite planes, respectively.

The transmittance peak at wavelength 3281 (Figure 3, IR spectra, arrow 1) was decreased in 3X collagen membranes, indicating the formation of O–H bonds. Moreover, the fingerprint area corroborated the identity of collagen in membranes. Peaks 1660 (Amide I band), 1627, 1635 (β-sheet 2ry structures of Amide I)**,** 1637 (triple helix), and 1679 (stretching C=O vibrations that are H bonded) were fused into a peak with least transmittance at 1635 (Figure 4, IR spectra, arrow 2). Peak 1635 indicating β-sheet secondary structures were correlated with the laminar structure shown in transversal SEM sections. The peak at 1535 (Figure 4, IR spectra, arrow 3) indicated Amide II, whereas the peak at 1240 (Figure 4, IR spectra, arrow 6) was characteristic of collagen. The contribution of peaks at 1446, 1396, and 1202 is seldom (or not at all) reported in the literature (Figure 4, IR spectra, arrows 4, 5, and 7). Peaks 1084 and 1029 (Figure 4, IR spectra, arrows 8 and 9) are related to nucleic acids. Peak 1084 corresponds to the

Preprints (www.preprints.org) | NOT PEER-REVIEWED | Posted: 30 May 2022 doi:10.20944/preprints202205.0396.v1

phosphodiester bonds of the phosphate/sugar backbone of nucleic acids, whereas peak 1029 was reported as corresponding to collagen and the phosphodiester groups of nucleic acids. Finally, the peaks at 565 and 527 (Figure 4, IR spectra, arrow 10) corresponded to phenyl group torsion. All peaks were intensified as collagen volume increased.

The membranes produced using our method were ~90% transparent in the visible light spectrum (Figure 4, Transmittance). The average transmittance for 1X membranes was 92.6%, whereas it was 94% for 2X and 89.21% for 3X membranes. Lower transmittance values were recorded at violet wavelengths (ranging from 380 to 450 nm); 1X CVM, 80.4%; 2X CVM, 82.98%; and 3X CVM, 77.56%. Moreover, 1X CVM yielded a transmittance peak of 99.6% at 560 nm and 2X CVM had a peak of 99% at 540 nm, both of which are in the green wavelength spectrum. In contrast, 3X CVM exhibited no peak but yielded higher transmittance values (94.7%) at 650 nm. Percent transmittance increased progressively and stabilized at 510 nm (1X) and 590 nm (2X and 3X). Increasing collagen concentration decreased transmittance by ~2.5% per added volume, with 1X CVM showing the highest percent transmittance. ANOVA indicated the presence of significant differences ($P \leq 0.001$) for 3X compared with 1X and 2X CVM.

The XRD patterns of pure collagen type 1 (1X, 2X, and 3X CVM) are shown in Figure 4, X-ray diffraction. All samples exhibited a typical broad hump around 22°, indicating that collagen was in an amorphous phase [22], [23]. A high-intensity peak was observed at 25.9°, which was related with the hydroxyapatite (HA) 002 plane. A shoulder of the HA 320 plane in the hump was shown at 39.8° compared with datasheet 9-432 from the Joint Committee of Powder Diffraction Standards. All samples showed a similar pattern, regardless of the content of collagen.

3.9 Wet lab with ex vivo model for surgical manipulation test

The *ex vivo* model using cow eyes was useful for the practicing of surgical procedures in the transplantation of the collagen membranes (Figure 5). 1X CVM were fragile and fragmented easily when manipulated surgically. 2X and 3X CVM were easier of surgically manipulation. Taken together with the cell adherence results, the 2X membranes were selected for further construct assembling and pilot transplantation.

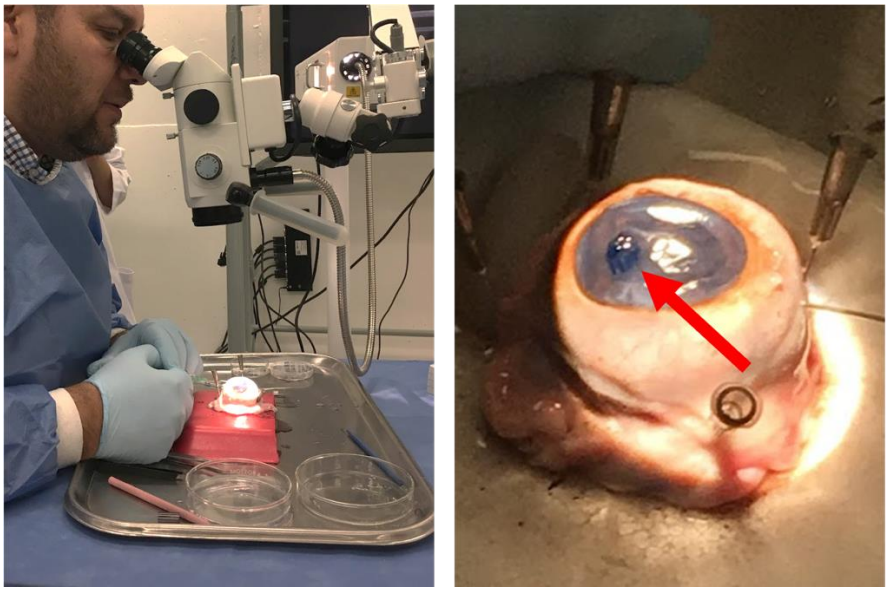

Preprints (www.preprints.org) | NOT PEER-REVIEWED | Posted: 30 May 2022 doi:10.20944/preprints202205.0396.v1

Figure 5. *Ex vivo* model for surgical manipulation test of collagen membranes. Manipulation of the model under the stereoscope (left). Membrane dyed with trypan blue transplanted into de anterior chamber of the *ex vivo* model (right).

3.10 Engineered corneal endothelium

After an overnight incubation, there were confluent zones of CEC over 2X CVM (Figure 6). However, the overall confluence was ~30% in all the membranes. Given that prior analysis demonstrated that the membrane allows cell proliferation, transplantation of the constructs to the animal model was conducted to evaluate the ability of the CECs to proliferate *in vivo* over the membrane and to restore the corneal clarity.

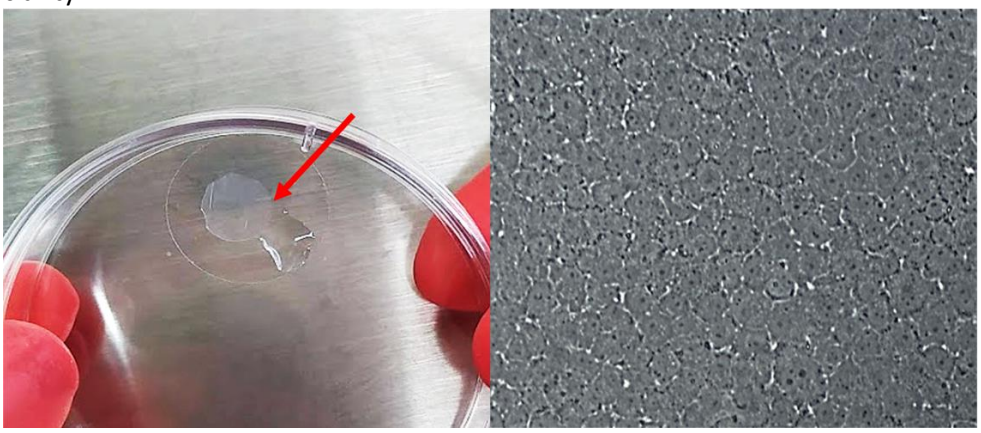

Figure 6. Engineered corneal endothelium (arrow): construct made of CVM and CECs (left). Microscopic view (20X) of CECs cultured over 2X CVM (right).

3.11 Pilot transplantation

All the eyes (7) that underwent Descemethorrexis developed corneal opacity after 5 minutes. The 4 eyes transplanted with CECs/CVM construct (experimental group) showed peripheral corneal clarity and

Preprints (www.preprints.org) | NOT PEER-REVIEWED | Posted: 30 May 2022 doi:10.20944/preprints202205.0396.v1

central opacity after 3 weeks that was consistent for the 90 days of the follow up. The 3 eyes transplanted with CVM (control group) showed full corneal opacity during the 4 weeks of follow up (**Figure 7**).

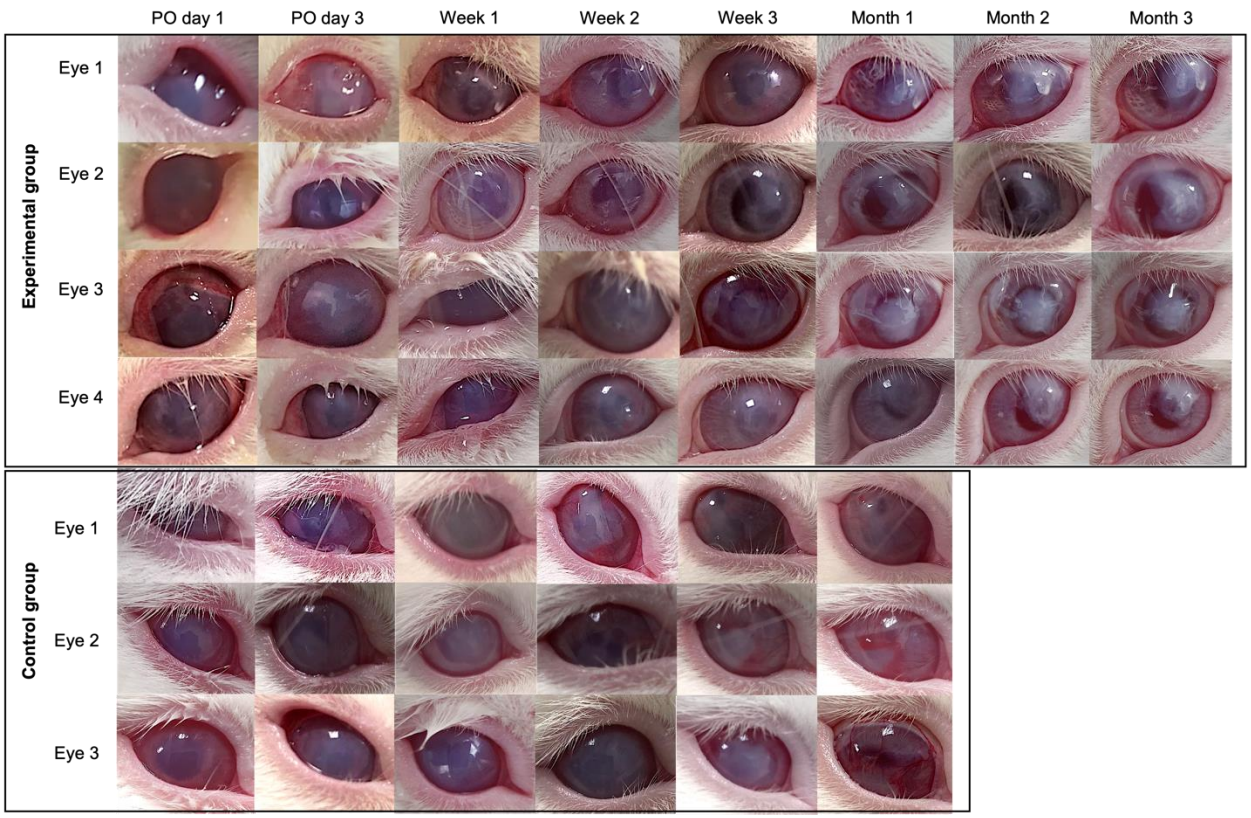

Figure 7. Postoperative follow up of eyes transplanted with CECs/CVM construct and with 2X CVM alone. The eyes with CECs/CVM transplant recovered peripheral transparency, while eyes transplanted with 2X CVM consistently showed edema.

The excised corneas transplanted with construct or CVM, showed the membrane adhered to the stroma. The endothelium of corneas transplanted with construct showed polygonal cells positive for ZO-1 and Na-K/ATPase by immunocytochemistry analysis throughout the tissue. Light microscopy showed polygonal

Preprints (www.preprints.org) | NOT PEER-REVIEWED | Posted: 30 May 2022 doi:10.20944/preprints202205.0396.v1

cells all over the collagen membranes of eyes transplanted with the constructs (Figure 8). No cells were observed in the eyes transplanted with the collagen membranes alone.

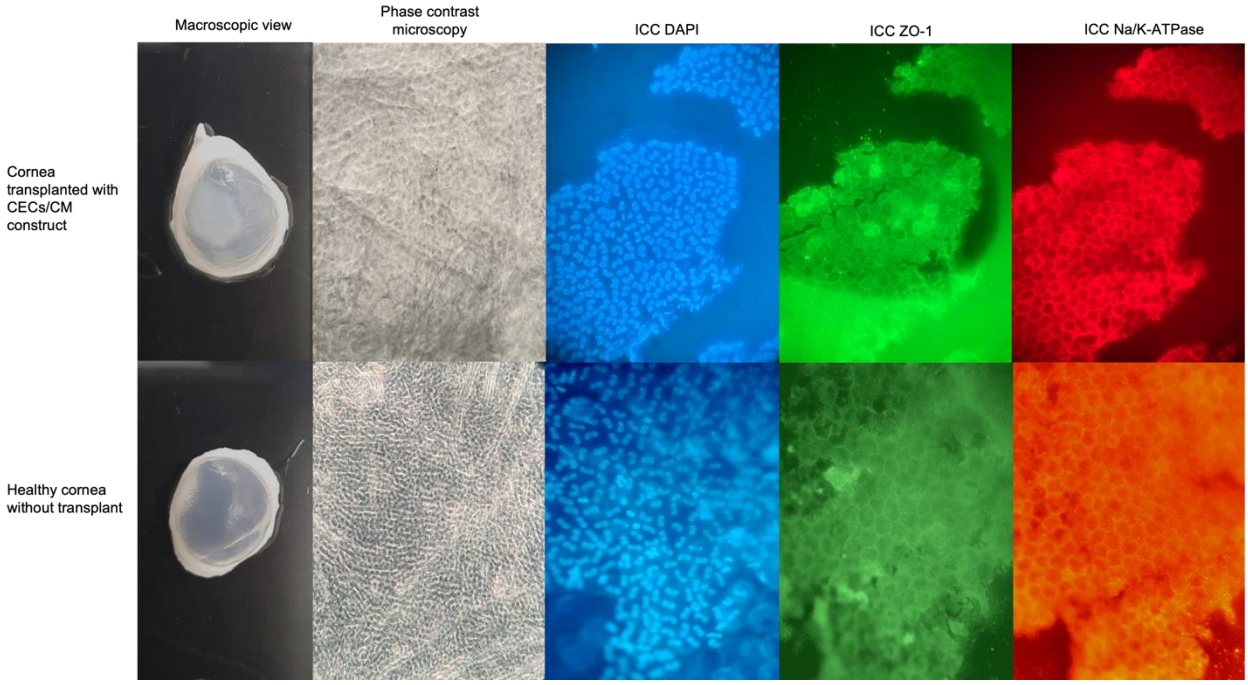

Figure 8. Macroscopic view of representative transplanted and healthy corneas and microscopical analysis: phase contrast microscopy showing corneal endothelium (10X) and immunocytochemistry (ICC) analysis showing the presence of the ZO-1 and Na/k-ATPase markers (20X).

Discussion

Collagen scaffolds possess beneficial properties that are widely studied for tissue engineering strategies. The methods reported to produce them include gelation, reverse dialysis, electrospinning, and lyophilization [14], [24]–[26], among others. The collagen concentration and the production process can be tailored to modify the scaffold properties depending on the tissue in which it is intended to be used. The vitrification process improves the mechanical properties of collagen scaffolds and provides optical clarity [14]. Although the biomedical potential of these membranes is well known, the available methods lack of fully detailed procedures, making it difficult to reproduce.

We describe a method to produce collagen scaffolds using common laboratory equipment and materials, providing a detailed procedure that can be tailored to produce scaffolds with properties according to the needs. We also demonstrated the biocompatibility and effectiveness of these membranes *in vitro* and in a preliminary *in vivo* model for corneal engineering. We used a matryoshka desiccation system that provided a stable RH and allowed the vitrification process. The RH variation was like that reported for commercial humidity chambers. The desiccation time yielded transparent membranes easy to remove from the plates.

 doi:10.20944/preprints202205.0396.v1

The width of the CVM relied on the time of desiccation more than on the collagen concentration. Our 1X membranes at 1 week of desiccation were not functional, they were too weak even to resist hydration for separation from the cast. Overall, our membranes were 3 to 16 times thinner than that reported previously using collagen [13], [15] and other materials such as amniotic membrane, human collagen, silk fibroin, hyaluronic acid, and decellularized extracellular matrix, which are 20-50 μm width [27]–[29].

Our SEM data showed randomly arranged fibrils at the surface of the membranes after short desiccation periods. The fibers observed here were larger by an order of magnitude, compared with the sizes of collagen membranes reported previously and resembled the early fibrils reported for collagen gels [14], [15], [23]. This is attributed to the different order of the neutralization and blending steps used for gel formation [30]. Moreover, the incubation conditions affect the increase in the thickness of fibrils: the lateral fusion of discrete (~4 nm) subunits leads to an increase in fibril diameter, followed by longitudinal growth [31]. Fibril bundling and total unification (greater fibril density and homogeneity) were observed when drying time was increased and high temperatures were used, leading to the production of the homogeneous and smooth surface observed in 1X, 2X, and 3X CVM. A similar non-fibrillar surface was reported in collagen membranes crosslinked with 1-ethyl-3-(3-dimethyl aminopropyl) carbodiimide (EDC) and N-hydroxysuccinimide (NHS) and UV [32], [33]. The transversal laminar arrangement is also conserved across collagen-based membranes produced using similar systems [15], [34].

The optical transparency of our membranes was higher than of the human cornea [35]. Even at similar collagen concentrations, the transmittance pattern of 1X and 2X CVM was different from those obtained using the different experimental conditions because of the peak detected at the green wavelength (around 550 nm). Transmittance patterns similar to that observed for our 3X CVM have been reported for other collagen membranes, combinations of silk–fibroin, hyaluronic acid, and fish-scale collagen scaffold [33] [14], [32]–[34], [36]–[38]. The increase in collagen deposition (i.e., membrane width) sets a light transmittance threshold and pattern [38]. Therefore, the tailoring of the ultrastructure of these membranes by changing desiccation conditions and collagen concentration allows the convenient adaptation of their optical transmittance.

FTIR and X Ray Diffraction analyses are not often provided in the characterization analysis of this type of scaffolds. However, they are useful in the demonstration of the crosslinking level of the collagen in the membrane, data pertaining to the origin of the collagen and desirable properties regarding biological responses, such as enhancement of mineralization, long-term degradation, and tissue integration [23], [30], [39].

The three types of CVM allowed the adhesion and growth of NIH3T3 cells, which is in accordance with previous findings [40]. Further surgical manipulation in the *ex vivo* model allowed to identify the most suitable for transplantation purposes. The 3X CVM was the most suitable for surgical implantation given its mechanical strength. However, CECs did not adhere easily on this type of membrane (data not shown). 2X CVM were chosen for transplantation *in vivo* given that

they allowed CECs adherence and ease surgically manipulation. Previous works report wet labs as cost-effective techniques for the acquisition of surgical abilities in the engineered corneal transplantation [41], [42].

Finally, the pilot transplantation of the CVM/CEC constructs *in vivo* showed that our CVM is suitable for surgical manipulation, adhere to the corneal stroma, and allows CECs proliferation *in situ* in a model of corneal opacity with high similarities to the human ocular physiology [20]. This is in contrast with the results previously reported using collagen membranes with higher width that showed low adherence to the corneal stroma and a low cell viability after transplantation [41]. Implanting of CVM/CECs partially restored the corneal clarity in our model, in contrast with the reported in previous research [43] in which total transparency was recovered. This can be explained by the lack of total cell confluency of CECs over CVM prior transplantation. Although CECs proliferated and covered all the CVM area, a fibrosis process might take place in the tissue faster than the CE recovering. As a pilot study, the transplantation demonstrated the overall higher characteristics of out vitrified CVM for corneal tissue engineering in contrast with previous studies [44], including transparency, biocompatibility, cell adherence and proliferation, mechanical strength for surgical manipulation, and stromal *in vivo* adherence.

Conclusion

Here we present a detailed and reproducible method to produce collagen scaffolds for tissue engineering. Using common laboratory equipment, we assembled a Matryoshka system that yielded CVM with superior characteristics of previously reported collagen membranes, including optical transparency (superior to that of the human cornea), is ultrathin (and the width can be tailored according to the needs of the tissue), biocompatibility, allows the cell adherence and proliferation, and is suitable for surgical manipulation. When implanted in the ocular anterior chamber, our CVM promoted corneal endothelial cells proliferation, attached to the stroma without interfering with the normal structure, function, nor causing adverse effects. Future preclinical studies will corroborate the ability of CVM as scaffold of CECs for the full restoration of corneal clarity.

Funding

This research was funded by CONACyT Grant PN6558.

Author Contributions:

Conceptualization, Judith Zavala and Jorge Eugenio Valdez-García; Data curation, María Montalvo-Parra, Denise Loya-García, Andres Bustamante-Arias, Guillermo Guerrero-Ramírez, César Calzada-Rodríguez, Guiomar Torres-Guerrero, Bestabé Hernández-Sedas, Italia Cárdenas-Rodríguez, Sergio Guevara-Quintanilla, Marcelo Salán-Flores, Miguel Hernández-Delgado, Salvador Garza-González, Mayra Gamboa-Quintanilla and Luis Villagómez-Valdez; Formal analysis, María Montalvo-Parra, Wendy Ortega-Lara, Denise Loya-García, Andres Bustamante-Arias, Guillermo Guerrero-Ramírez, César Calzada-Rodríguez, Guiomar Torres-Guerrero, Bestabé Hernández-Sedas, Italia Cárdenas-Rodríguez, Sergio Guevara-Quintanilla, Marcelo Salán-Flores, Miguel Hernández-Delgado, Salvador Garza-González, Mayra Gamboa-Quintanilla and Luis Villagómez-Valdez; Funding acquisition, Jorge Eugenio Valdez-García; Investigation, María Montalvo-Parra, Judith Zavala and Jorge Eugenio Valdez-García; Methodology, María Montalvo-Parra, Denise Loya-García, Andres Bustamante-Arias, Guillermo Guerrero-Ramírez, César Calzada-

Rodríguez, Guiomar Torres-Guerrero, Bestabé Hernández-Sedas, Italia Cárdenas-Rodríguez, Sergio Guevara-Quintanilla, Marcelo Salán-Flores, Miguel Hernández-Delgado, Salvador Garza-González, Mayra Gamboa-Quintanilla and Luis Villagómez-Valdez; Project administration, Judith Zavala; Resources, Wendy Ortega-Lara, Judith Zavala and Jorge Eugenio Valdez-García; Supervision, Judith Zavala and Jorge Eugenio Valdez-García; Validation, María Montalvo-Parra, Wendy Ortega-Lara, Denise Loya-García, Andres Bustamante-Arias, Guillermo Guerrero-Ramírez, César Calzada-Rodríguez, Guiomar Torres-Guerrero, Bestabé Hernández-Sedas, Italia Cárdenas-Rodríguez, Sergio Guevara-Quintanilla, Marcelo Salán-Flores, Miguel Hernández-Delgado, Salvador Garza-González, Mayra Gamboa-Quintanilla and Luis Villagómez-Valdez; Visualization, María Montalvo-Parra; Writing – original draft, María Montalvo-Parra and César Calzada-Rodríguez; Writing – review & editing, Judith Zavala.

Conflict of interest

The authors declare no conflict of interest

References

[1] R. Girlanda, "Deceased organ donation for transplantation: Challenges and opportunities," *World Journal of Transplantation*, vol. 6, no. 3, p. 451, Sep. 2016, doi: 10.5500/WJT.V6.I3.451.

[2] "Organ donation and transplants - PAHO/WHO | Pan American Health Organization." https://www.paho.org/en/topics/organ-donation-and-transplants (accessed May 25, 2022).

[3] C. Dong and Y. Lv, "Application of Collagen Scaffold in Tissue Engineering: Recent Advances and New Perspectives," *Polymers (Basel)*, vol. 8, no. 2, 2016, doi: 10.3390/POLYM8020042.

[4] A. D. Nocera, R. Comín, N. A. Salvatierra, and M. P. Cid, "Development of 3D printed fibrillar collagen scaffold for tissue engineering," *Biomed Microdevices*, vol. 20, no. 2, Jun. 2018, doi: 10.1007/S10544-018-0270-Z.

[5] S. N. Park, J. C. Park, H. O. Kim, M. J. Song, and H. Suh, "Characterization of porous collagen/hyaluronic acid scaffold modified by 1-ethyl-3-(3-dimethylaminopropyl)carbodiimide cross-linking," *Biomaterials*, vol. 23, no. 4, pp. 1205–1212, Feb. 2002, doi: 10.1016/S0142-9612(01)00235-6.

[6] A. Nakada *et al.*, "Manufacture of a weakly denatured collagen fiber scaffold with excellent biocompatibility and space maintenance ability," *Biomed Mater*, vol. 8, no. 4, 2013, doi: 10.1088/1748-6041/8/4/045010.

[7] E. E. Antoine, P. P. Vlachos, and M. N. Rylander, "Tunable collagen I hydrogels for engineered physiological tissue micro-environments," *PLoS ONE*, vol. 10, no. 3, Mar. 2015, doi: 10.1371/JOURNAL.PONE.0122500.

[8] X. Chen *et al.*, "Functional Multichannel Poly(Propylene Fumarate)-Collagen Scaffold with Collagen-Binding Neurotrophic Factor 3 Promotes Neural Regeneration After Transected Spinal Cord Injury," *Adv Healthc Mater*, vol. 7, no. 14, Jul. 2018, doi: 10.1002/ADHM.201800315.

[9] J. A. Inzana *et al.*, "3D printing of composite calcium phosphate and collagen scaffolds for bone regeneration," *Biomaterials*, vol. 35, no. 13, pp. 4026–4034, Apr. 2014, doi: 10.1016/J.BIOMATERIALS.2014.01.064.

[10] A. Sensini *et al.*, "Tendon Fascicle-Inspired Nanofibrous Scaffold of Polylactic acid/Collagen with Enhanced 3D-Structure and Biomechanical Properties," *Scientific Reports 2018 8:1*, vol. 8, no. 1, pp. 1–15, Nov. 2018, doi: 10.1038/s41598-018-35536-8.

[11] U. Bertram *et al.*, "Vascular Tissue Engineering: Effects of Integrating Collagen into a PCL Based Nanofiber Material," *Biomed Res Int*, vol. 2017, 2017, doi: 10.1155/2017/9616939.

[12] R. J. F. C. do Amaral *et al.*, "Functionalising Collagen-Based Scaffolds With Platelet-Rich Plasma for Enhanced Skin Wound Healing Potential," *Frontiers in Bioengineering and Biotechnology*, vol. 7, p. 371, Dec. 2019, doi: 10.3389/FBIOE.2019.00371/BIBTEX.

[13] T. Takezawa, K. Ozaki, A. Nitani, C. Takabayashi, and T. Shimo-Oka, "Collagen vitrigel: a novel scaffold that can facilitate a three-dimensional culture for reconstructing organoids," *Cell Transplant*, vol. 13, no. 4, pp. 463–473, 2004, doi: 10.3727/000000004783983882.

[14] X. Calderón-Colón *et al.*, "Structure and properties of collagen vitrigel membranes for ocular repair and regeneration applications," *Biomaterials*, vol. 33, no. 33, pp. 8286–8295, Nov. 2012, doi: 10.1016/J.BIOMATERIALS.2012.07.062.

[15] W. M. I. Ambrose *et al.*, "Collagen Vitrigel membranes for the in vitro reconstruction of separate corneal epithelial, stromal, and endothelial cell layers," *J Biomed Mater Res B Appl Biomater*, vol. 90, no. 2, pp. 818–831, 2009, doi: 10.1002/JBM.B.31351.

[16] E. E. Antoine, P. P. Vlachos, and M. N. Rylander, "Review of Collagen I Hydrogels for Bioengineered Tissue Microenvironments: Characterization of Mechanics, Structure, and Transport," *Tissue Engineering. Part B, Reviews*, vol. 20, no. 6, p. 683, Dec. 2014, doi: 10.1089/TEN.TEB.2014.0086.

[17] S. J. Hollister, "Scaffold engineering: a bridge to where?," *Biofabrication*, vol. 1, no. 1, 2009, doi: 10.1088/1758-5082/1/1/012001.

[18] M. D. Montalvo-Parra *et al.*, "Experimental design of a culture approach for corneal endothelial cells of New Zealand white rabbit," *Heliyon*, vol. 6, no. 10, 2020, doi: 10.1016/j.heliyon.2020.e05178.

[19] C.-A. Rodríguez-Barrientos *et al.*, "Arresting proliferation improves the cell identity of corneal endothelial cells in the New Zealand rabbit," *Molecular Vision*, vol. 25, 2019.

[20] J. E. Valdez-Garcia, J. F. Lozano-Ramirez, and J. Zavala, "Adult white New Zealand rabbit as suitable model for corneal endothelial engineering," *BMC Research Notes*, vol. 8, no. 1, 2015, doi: 10.1186/s13104-015-0995-1.

[21] C. A. Schneider, W. S. Rasband, and K. W. Eliceiri, "NIH Image to ImageJ: 25 years of image analysis," *Nature Methods*, vol. 9, no. 7, pp. 671–675, 2012, doi: 10.1038/nmeth.2089.

[22] Y. Tanaka *et al.*, "Transparent, tough collagen laminates prepared by oriented flow casting, multi-cyclic vitrification and chemical cross-linking," *Biomaterials*, vol. 32, no. 13, pp. 3358–3366, 2011, doi: https://doi.org/10.1016/j.biomaterials.2010.11.011.

[23] K. E. Kadler, D. F. Holmes, J. A. Trotter, and J. A. Chapman, "Collagen fibril formation," *Biochem J*, vol. 316 (Pt 1), no. Pt 1, pp. 1–11, May 1996, doi: 10.1042/bj3160001.

[24] M. Achilli and D. Mantovani, "Tailoring Mechanical Properties of Collagen-Based Scaffolds for Vascular Tissue Engineering: The Effects of pH, Temperature and Ionic Strength on Gelation," *Polymers 2010, Vol. 2, Pages 664-680*, vol. 2, no. 4, pp. 664–680, Dec. 2010, doi: 10.3390/POLYM2040664.

[25] G. S. Offeddu, J. C. Ashworth, R. E. Cameron, and M. L. Oyen, "Multi-scale mechanical response of freeze-dried collagen scaffolds for tissue engineering applications," *J Mech Behav Biomed Mater*, vol. 42, pp. 19–25, Feb. 2015, doi: 10.1016/J.JMBBM.2014.10.015.

[26] B. Zhu, W. Li, R. v Lewis, C. U. Segre, and R. Wang, "E-Spun Composite Fibers of Collagen and Dragline Silk Protein: Fiber Mechanics, Biocompatibility, and Application in Stem Cell Differentiation," *Biomacromolecules*, vol. 16, no. 1, pp. 202–213, Jan. 2015, doi: 10.1021/bm501403f.

[27] T. Huibertus van Essen *et al.*, "A fish scale-derived collagen matrix as artificial cornea in rats: properties and potential," *Invest Ophthalmol Vis Sci*, vol. 54, no. 5, pp. 3224–3233, 2013, doi: 10.1167/IOVS.13-11799.

[28] Y. Liu, L. Ren, and Y. Wang, "Crosslinked collagen-gelatin-hyaluronic acid biomimetic film for cornea tissue engineering applications," *Mater Sci Eng C Mater Biol Appl*, vol. 33, no. 1, pp. 196–201, Jan. 2013, doi: 10.1016/J.MSEC.2012.08.030.

[29] N. Vázquez *et al.*, "Human Bone Derived Collagen for the Development of an Artificial Corneal Endothelial Graft. In Vivo Results in a Rabbit Model," *PLoS One*, vol. 11, no. 12, Dec. 2016, doi: 10.1371/JOURNAL.PONE.0167578.

[30] D. F. Holmes, M. J. Capaldi, and J. A. Chapman, "Reconstitution of collagen fibrils in vitro; the assembly process depends on the initiating procedure," *International Journal of Biological Macromolecules*, vol. 8, no. 3, pp. 161–166, Jun. 1986, doi: 10.1016/0141-8130(86)90020-6.

[31] D. L. Christiansen, E. K. Huang, and F. H. Silver, "Assembly of type I collagen: fusion of fibril subunits and the influence of fibril diameter on mechanical properties," *Matrix Biol*, vol. 19, no. 5, pp. 409–420, 2000, doi: 10.1016/S0945-053X(00)00089-5.

[32] M. Nair, Y. Calahorra, S. Kar-Narayan, S. M. Best, and R. E. Cameron, "Self-assembly of collagen bundles and enhanced piezoelectricity induced by chemical crosslinking†," *Nanoscale*, vol. 11, no. 32, p. 15120, Aug. 2019, doi: 10.1039/C9NR04750F.

[33] N. Vázquez *et al.*, "Human Bone Derived Collagen for the Development of an Artificial Corneal Endothelial Graft. In Vivo Results in a Rabbit Model," *PLoS One*, vol. 11, no. 12, Dec. 2016, doi: 10.1371/JOURNAL.PONE.0167578.

[34] K. Long *et al.*, "Improving the mechanical properties of collagen-based membranes using silk fibroin for corneal tissue engineering," *J Biomed Mater Res A*, vol. 103, no. 3, pp. 1159–1168, Mar. 2015, doi: 10.1002/JBM.A.35268.

[35] E. M. Beems and J. A. van Best, "Light transmission of the cornea in whole human eyes," *Exp Eye Res*, vol. 50, no. 4, pp. 393–395, 1990, doi: 10.1016/0014-4835(90)90140-P.

[36] K. Long *et al.*, "Improving the mechanical properties of collagen-based membranes using silk fibroin for corneal tissue engineering," *J Biomed Mater Res A*, vol. 103, no. 3, pp. 1159–1168, Mar. 2015, doi: 10.1002/JBM.A.35268.

[37] T. Huibertus van Essen *et al.*, "A fish scale-derived collagen matrix as artificial cornea in rats: properties and potential," *Invest Ophthalmol Vis Sci*, vol. 54, no. 5, pp. 3224–3233, 2013, doi: 10.1167/IOVS.13-11799.

[38] Y. Tanaka *et al.*, "Transparent, tough collagen laminates prepared by oriented flow casting, multi-cyclic vitrification and chemical cross-linking," *Biomaterials*, vol. 32, no. 13, pp. 3358–3366, May 2011, doi: 10.1016/J.BIOMATERIALS.2010.11.011.

[39] S. N. Park, J. C. Park, H. O. Kim, M. J. Song, and H. Suh, "Characterization of porous collagen/hyaluronic acid scaffold modified by 1-ethyl-3-(3-dimethylaminopropyl)carbodiimide cross-linking," *Biomaterials*, vol. 23, no. 4, pp. 1205–1212, Feb. 2002, doi: 10.1016/S0142-9612(01)00235-6.

[40] J. S. Choi *et al.*, "In vitro evaluation of the interactions between human corneal endothelial cells and extracellular matrix proteins," *Biomed Mater*, vol. 8, no. 1, 2013, doi: 10.1088/1748-6041/8/1/014108.

[41] D. Spinozzi *et al.*, "In Vitro Evaluation and Transplantation of Human Corneal Endothelial Cells Cultured on Biocompatible Carriers," *Cell Transplantation*, vol. 29, May 2020, doi: 10.1177/0963689720923577.

[42] A. Srirampur and T. Mansoori, "A simplified ex vivo model to learn the correct orientation of Descemet membrane endothelial graft," *Indian Journal of Ophthalmology*, vol. 69, no. 1, pp. 151–152, Jan. 2021, doi: 10.4103/IJO.IJO_1720_19.

[43] T. Mimura *et al.*, "Cultured Human Corneal Endothelial Cell Transplantation with a Collagen Sheet in a Rabbit Model," *Investigative Ophthalmology & Visual Science*, vol. 45, no. 9, pp. 2992–2997, Sep. 2004, doi: 10.1167/IOVS.03-1174.

[44] M. Ahearne, J. Fernández-Pérez, S. Masterton, P. W. Madden, and P. Bhattacharjee, "Designing Scaffolds for Corneal Regeneration," *Advanced Functional Materials*, vol. 30, no. 44, Oct. 2020, doi: 10.1002/ADFM.201908996.